Integrated stopped-flow device for the study of porous materials using hyperpolarized ^{129}Xe NMR

Jing Li, Estelle Léonce, Corentin Coutellier, Céline Boutin, Kévin Chighine, Charles Rivron, Anne Davidson, Patrick Berthault

An integrated stopped-flow device for the study of porous materials using hyperpolarized ^{129}Xe NMR

Jing Li,‡ Estelle Léonce,‡ Corentin Coutellier,‡ Céline Boutin,‡ Kévin Chighine,‡ Charles Rivron,‡ Anne Davidson,§ and Patrick Berthault‡*

‡ NIMBE, CEA, CNRS, UNIVERSITE DE PARIS SACLAY, CEA SACLAY, 91191 GIF-SUR-YVETTE, FRANCE

§ LABORATOIRE DE REACTIVITE DE SURFACE, SORBONNE UNIVERSITES, UPMC UNIVERSITE PARIS 06, UMR CNRS 7197, 4 PLACE JUSSIEU, 75005 PARIS, FRANCE

* Corresponding author. E-mail address: patrick.berthault@cea.fr

ABSTRACT: A simple, low-cost and efficient device is proposed for the study of porous materials via NMR using small gas probes. Mainly built through additive manufacturing and being equipped with a radiofrequency solenoid micro-coil, it only requires tiny quantities of porous and/or gas and is particularly suited for hyperpolarized xenon. The performances of this device have been accessed on a commercial sample of MCM-41 exhibiting multi-porosity. Both the delivery mode of hyperpolarized xenon and the stopped-flow system are judged efficient according to 2D ^{129}Xe self-diffusion and EXSY experiments.

INTRODUCTION

^{129}Xe NMR is widely used for in-depth studies of materials with micro- and nano-porosity, due to its fast diffusivity and the wide range of chemical shift the monoatomic species can take. It is well suited to complement N_2 sorption analysis, X-ray diffraction, and high-resolution transmission electron microscopy. The xenon chemical shift can be related to the void space in the absence of paramagnetic components, in accordance with the Ito-Fraissard relationship:[1]

$$\delta_{obs} = \delta_0 + \delta_S + \delta_{Xe} + \delta_{SAS} \qquad (1)$$

where δ_0 is the virtual Xe chemical shift at 0 atm; δ_S arises from the interaction between the gas and the material surface. The δ_{Xe} term is linked to the Xe-Xe collisions and is related to Xe concentration. The fourth term δ_{SAS} appears when strong adsorption sites are present.

However, the use of thermally polarized xenon requires long experiment times due to its low signal-to-noise ratio (SNR) and quite slow longitudinal relaxation. Moreover, at high xenon pressure, the δ_{Xe} term outweighs all others, making it sometimes difficult to explore porous surfaces using this method. To overcome the lack of sensitivity and thereby work with lower pressure, xenon nuclear spin populations can be transiently unbalanced by transfer from a more ordered system such as photons or electrons. This is the basis of the two popular hyperpolarized methods, Spin-Exchange Optical Pumping (SEOP)[2] and Dynamic Nuclear Polarization (DNP).[3]

However, the transient and non-easily reproducible character of the hyperpolarization renders difficult the recording of some classical 1D and 2D experiments. The - often unavoidable - fluctuating level of magnetization poses problems for quantifying the results obtained, whatever a batch[4] or on-flow[5] production of hyperpolarized xenon is used. While for porous materials, it has already been shown possible to record 2D exchange (EXSY) experiments[6,7,8,9,10] with hyperpolarized xenon, there is place for a simple and robust setup decorrelating the production of hyperpolarized gas from its use.

Here a disposable 3D-printed insert pluggable on a micro-imaging probehead basis itself installed in a narrow-bore NMR magnet is presented. The role of the device is to enable the automated delivery of hyperpolarized xenon gas into the porous material to be studied. Its principle derives from our previous NMR setups, intended either for the enrichment of solutions in hyperpolarization[11] or for the study of slowly relaxing nuclei,[12] but this disposable device (one insert for one sample) is even of greater simplicity and ease of use, its main advantage lying in its high versatility.

For assessing the performance of this setup for 1D and 2D hyperpolarized ^{129}Xe NMR experiments, a commercial sample of porous silica, MCM-41, exhibiting a multimodal porosity, is used.

DESCRIPTION OF THE DEVICE AND OPERATION MODE

Fig.1a describes the stopped flow system we built. An aluminum plate supports a programmable non-magnetic syringe pump on top of the magnet. As described in ref. 11, the syringe (1) contains an inert gas such as nitrogen to serve as carrier gas. Between the syringe and the glass serpentine containing hyperpolarized xenon (7), a first pneumatic valve (2) and a 3-way valve (4) are installed. A

pump (16) creates a vacuum upstream (5) and downstream (9) of the glass serpentine, according to the positions of the 3-way valves (4) and (10). This prevents dioxygen in parts (5) and (9) to collide with Xe, and depolarize it.

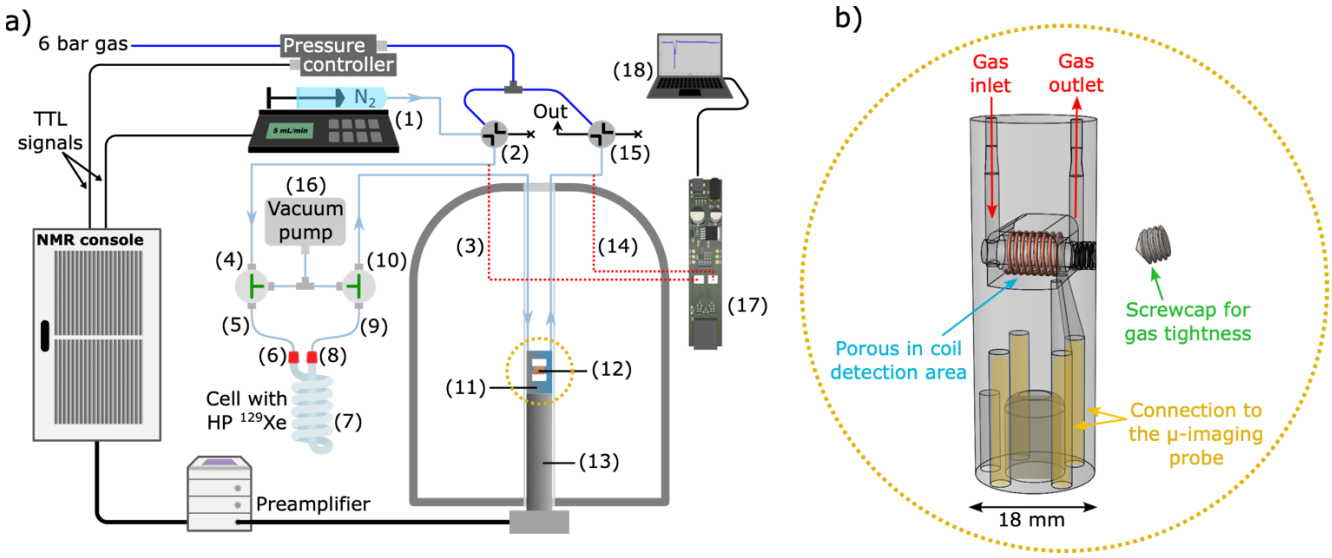

Figure 1. a) Schematics of the stopped-flow system for hyperpolarized ^{129}Xe NMR experiments on porous materials. For the meaning of numbers (1) to (18), see text. b) Drawing of the NMR insert plugged onto the micro-imaging probe basis. A copper solenoid coil is wrapped around the sample chamber, in close proximity to the porous material.

The NMR insert (11) made by 3D printing, except for the copper solenoid (12) and the brass connectors, is shown in Fig. 1b. Note that the solenoid coil ensures both RF emission and detection. Conversely to the developments proposed by McDonnell et al.,[13] no remote detection is used here. Rather, high sensitivity is expected due to the excellent filling factor, the copper coil being wrapped as close as possible to the sample chamber of diameter 2 mm. Porous volumes on the order of 25 mm^3 can thus be used. The insert is electrically plugged on a commercial micro-imaging probehead (13).

The gas is controlled to cross the chamber containing the porous material. The inlet and outlet pipes are controlled by two pneumatic valves (2 and 15) driven in the NMR sequence through TTL signals. When the pneumatic valves are under pressure of control gas, they are closed and the xenon flow is stopped. When there is no pressure, the pneumatic valves are open and xenon can flow through the circuit, as it is synchronized with the action of the syringe (also driven in the NMR sequence). The pressure is monitored upstream (3) and downstream (14) of the porous material via a dedicated homebuilt device (17). The data of the two pressure sensors are stored on a laptop (18) via a python homemade GUI. Full description of this pressure device and other details are given in the Experimental Section and in the Supporting Information (Figs. S1 and S2).

The instructions of use are the following. Before plugging of the insert (11) on the probe basis (13) and installation of the ensemble in the NMR magnet, the porous is manually introduced in the chamber. Then, a 3D-printed screwcap closes the assembly, but still allows gas to flow through the porous material. The gas inlet and outlet pipes in PEEK are connected to the circuit, then the completed probe is inserted into the magnet and all rf connections are made. Hyperpolarized xenon is transported from the optical pumping room to the NMR spectrometer, frozen in the glass serpentine (7) equipped with screwcaps (6, 8), itself immersed in liquid nitrogen, in the presence of a magnetic field of a few kilogausses. In the fringe field of the NMR magnet the glass serpentine is heated by immersion in hot water. Here xenon sublimates, and the glass serpentine is placed on top of the NMR magnet in a fringe field of ca. 200 G, where it is connected between the two 3-way valves (4) and (10). Vacuum is then made upstream (5) and downstream (9) of the closed glass serpentine. Then, the valves (4) and (10) are turned to close the vacuum access (16) and the two screw caps of the serpentine are open to allow the gas flow along the line (2)-(4)-(5)-(6)-(7)-(8)-(9)-(10)-(11)-(15). At this step, the NMR acquisition can start.

The NMR pulse sequence (for example, that of Fig. S6 or S7), starts by triggering both the pneumatic valves and the syringe pump.

Among the many advantages of such a configuration, the volume of xenon produced does not need to be large, the gas remains in a magnetic field sufficient for its depolarization time to be long, and recovering the xenon used is easy at the output of the second pneumatic valve.

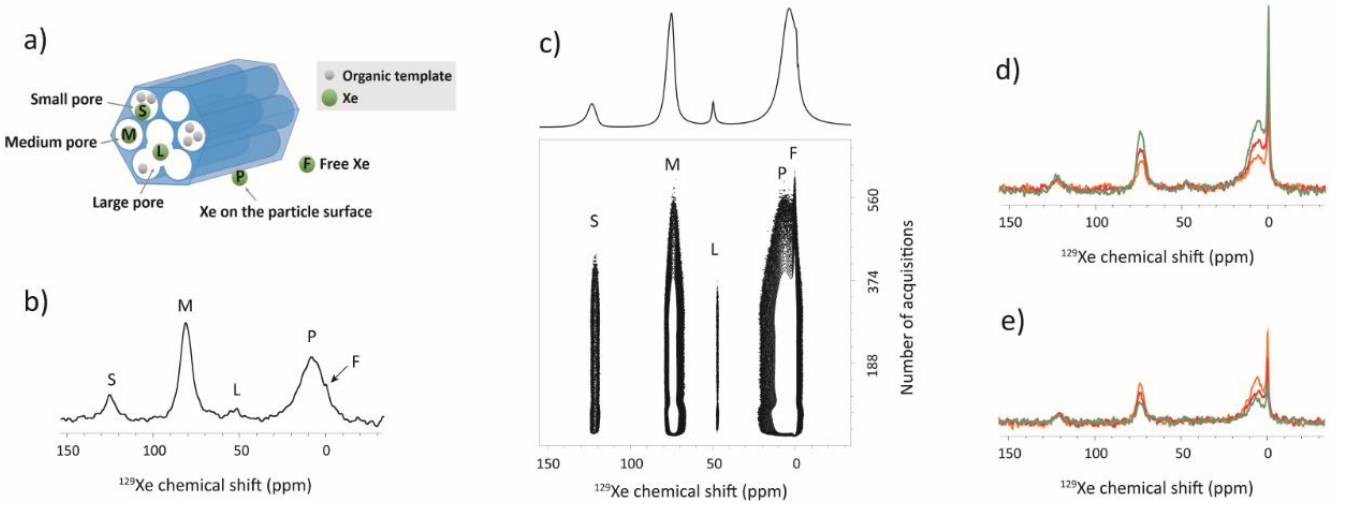

Figure 2. a) Schematic illustration of MCM-41 with indication of the pore type labels. b) ^{129}Xe NMR spectrum of thermally polarized xenon, acquired in 53 min at 293 K, with MCM-41 containing residual organic template arising from synthesis. c) Contour plot of a series of hyperpolarized ^{129}Xe spectra acquired each second at 298 K (the projection is displayed on top); d) First three ^{129}Xe spectra upon arrival of the hyperpolarized xenon in the experiment shown in c), in the order orange then red, then green and e) the last ^{129}Xe spectra recorded with hyperpolarized xenon (end of the flush) (orange: row 470, red: row 500 and green: row 527).

STUDY OF THE MCM-41 MATERIAL

The performances of this setup were assessed on a commercial MCM-41 sample by using hyperpolarized xenon in continuous or stopped-flow mode, and the results were compared to the thermally polarized xenon spectra acquired in static mode in an NMR tube. MCM-41 is a silicate material, presenting a hierarchical mesoporous structure with 2D hexagonal phase (Fig. 2a),[14] widely used as a catalyst[15] and adsorbent.[16] The surface properties of MCM-41 have often been characterized by hyperpolarized ^{129}Xe NMR, in particular through variable temperature experiments.[17,18]

According to the N_2 sorption result (see Fig. S3 and Table S1 of the Supporting Information), the MCM-41 we used has a Brunauer–Emmett–Teller (BET) specific surface of 886 m^2/g, a Density Functional Theory (DFT) surface area of 1308 m^2/g, a major Barrett-Joyner-Halenda (BJH) mesopore size of 2.3 nm and micropores in the range of 0.6-1.2 nm obtained from DFT. This material is MCM-41 still containing the surfactant template from its synthesis, as indicated by its multi-porosity.[19] Indeed, calcination at 900°C for 7 hours gave the ^{129}Xe spectrum shown in Fig. S4. The multi-porosity before calcination is perfect to assess the performance of our device.

Firstly, a ^{129}Xe spectrum was recorded in 640 scans (20 min) at 293 K with a sample of MCM-41 powder and 1.5 bar of thermally polarized (TP) xenon in a 5-mm NMR tube (Fig. 2b). It was used for comparing to the spectrum obtained with laser-polarized xenon. For the laser-polarized ^{129}Xe NMR experiment, a continuous flow rate of 3 mL/min was set on the syringe pump, corresponding to a rate of 1.6 cm/s in the NMR detection region. The hyperpolarized (HP) ^{129}Xe continuous flow-spectra (Fig. 2c) were acquired by looping 512 times of a {pulse-acquisition} sequence. A small flip angle pulse of about 5° was applied. The delay between two acquisitions was 1 s. Comparing the highest-intensity hyperpolarized spectrum (1 line, i. e. 1 scan) with the thermal spectrum (obtained in 640 scans with 90° pulses), the gain in signal-to-noise ratio is ca. 7.

The spectra acquired with thermally polarized and hyperpolarized gases look very similar: four peaks are observed. When Xe gas is adsorbed into this porous material which does not contain strong adsorbing sites, according to Eq. (1) the ^{129}Xe chemical shifts of the different sites are strongly related to the δ_s term. The δ_s term is inversely proportional to the pore size,[20] and thus the smallest pore has the highest δ_{obs} value. The peak at ca. 0 ppm is free Xe gas out of particles (denoted peak F). A broad peak appears at ca. 10 ppm (peak P); it results from the xenon population from the bulk in fast exchange with the particle surface.[21] A signal – narrow and of low intensity - appears at ca. 50 ppm. It corresponds to large pores (peak L). This may be the defective sites of the MCM-41, resulted from partial breakage of Si-O-Si bonds (here denoted as defective pore).[22] A small amount of large mesopores in the range of 4 to 10 nm were also found from the pore size distribution extracted from Barrett-Joyner-Halenda (BJH) desorption analysis (Fig. S3 and Table S1). The predominating signal at around 75 ppm corresponds to the 2D hexagonal, constant diameter, mesopores in MCM-41, labelled as M. This pore is assumed to be the pore centred at 2.3 nm on the BJH pore size distribution. A fourth signal, labelled S, appears at around 123 ppm, corresponding to xenon in partially clogged pores. The presence of nanopores were also confirmed by the DFT analysis of N_2 sorption. This nano-scaled space is presumably hexagonal mesopores with remaining organic template for synthesis.

With our device, it is also possible to extract the information about pore accessibility from the hyperpolarized xenon continuous flow spectra. Figure 2d displays the first three ^{129}Xe spectra recorded on arrival of hyperpolarized xenon. Remarkably, in this early phase the ratio of the integral signal intensity between the S peak and the M and L peaks diminishes with time. Xenon penetrates all pores in a similar way, and as its quantity increases, after filling

all S nanopores, it increases its filling of M and L pores. Conversely, in the last part of the xenon introduction (Fig. 2e), the integral signal intensity ratio S to (L+M) increases with time.

In order to obtain more complete information on pore size, xenon accessibility and pore connections, the use of self-diffusion and exchange experiments can be invaluable. However, one prerequisite is to calibrate the rf pulses, which is no trivial matter, and another is to be able to stop the gas flow as required. For the latter purpose, we installed two pneumatic valves at the top of the magnet, one positioned on the xenon inlet pipe and the other on the xenon outlet (see Fig. 1). The gas pressure supply to actuate the valves was controlled in the NMR pulse sequence.

With such a device it becomes easier to calibrate the rf pulses. In order to calibrate the ^{129}Xe rf channel of the NMR insert in the presence of a porous, the following procedure was used. For one xenon batch (i.e. between two openings of the pressure-driven valves), a series of 16 or 32 {pulse – acquisition} sequences was then performed, with a given θ pulse flip angle (θ < 90°). The resulting signal evolution could be fitted against the theoretical recursive equation to extract θ, in a procedure analogue to that of Norquay et al.[23] (Fig. 3b):

$$M_i = M_{i-1} cos\theta \qquad (2)$$

In these experiments the very short interscan delay (62 ms) ensures that longitudinal relaxation can be neglected. Figure 3 displays such a calibration, as well as the verification experiment containing only 90° pulses (Fig. 3c). The fact that, after each syringe push, only the first scan contains signal in this last experiment proves that the 90° angle has indeed been reached, since the xenon in the porous region has been totally depolarized at once.

^{129}Xe self-diffusion experiments. With this calibration in hand, it is possible to perform ^{129}Xe self-diffusion experiments at room temperature. Two stimulated echo experiments with different diffusion times (Δ) and gradient lengths (δ) have been recorded; they contained a linear ramp of 16 gradient strengths (g) each, from 4 G/cm to 90 G/cm.

After each xenon renewal and after gas flow has stopped, the sequence is repeated. As the level of magnetization is prone to fluctuate (both the polarization and the concentration parts), a reference experiment consisting in a simple acquisition after a small flip angle excitation pulse is interleaved with the self-diffusion experiment (thus for each gradient value), see Fig. 4a.

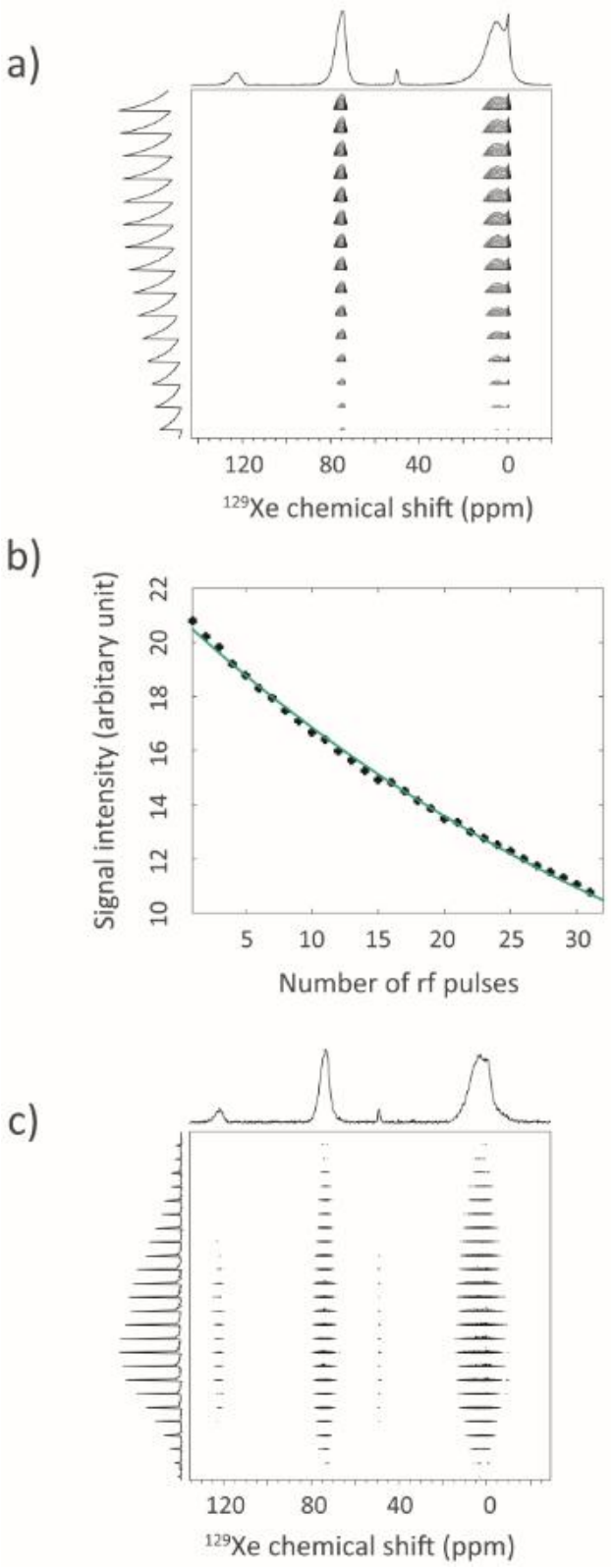

Figure 3. Radiofrequency pulses calibration procedure. In a) a series of ^{129}Xe spectra obtained using the stopped-flow system after a read pulse of unknown flip angle θ (θ < 90°) is displayed. 16 pushes made up the experiment, and for each of them 32 FIDs were recorded at 1 s interval with the sequence {Pulse θ – acquisition}. b) The plot of the signal integral as a function of the index of the pulse and the fit against the theoretical function gives θ. c) As a verification, an experiment with θ = 90° is displayed.

A qualitative comparison between the self-diffusion experiment (Fig. 4c) and the repetition of single pulses (Fig. 4b) reveals some interesting features. First, in the self-diffusion experiment, peak P does not appear. Even if a stimulated echo sequence has been used, this could be due to very fast transverse relaxation, probably due to the interaction with the particle surface. Second, peaks F and L are observed to quickly decrease while peaks S and M do not decrease so much. This means that the free gas and the gas in large pores diffuse faster than the ^{129}Xe gas in small and medium pores, as expected.

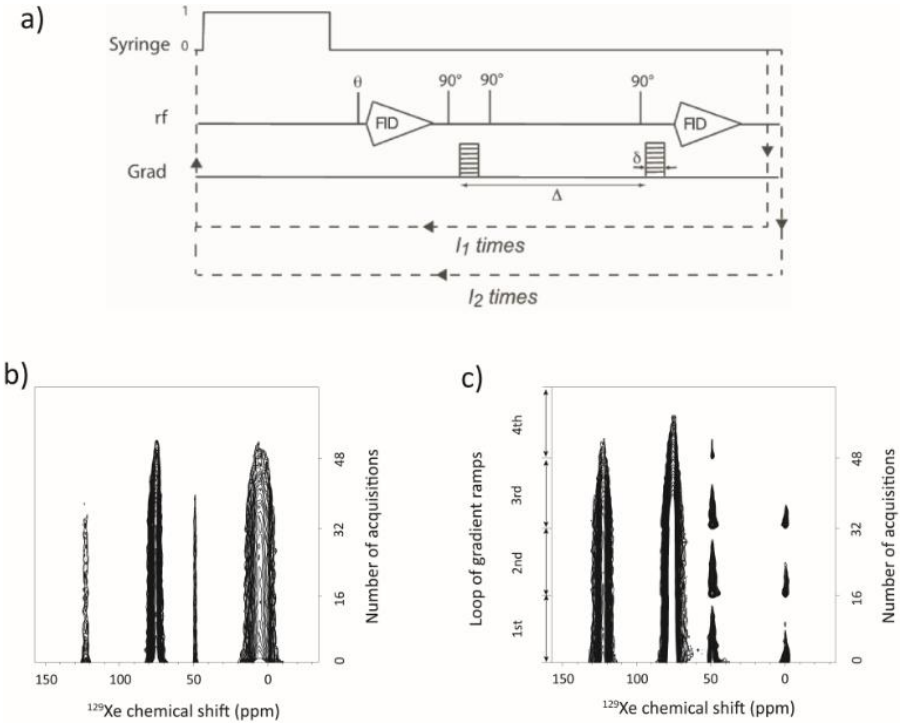

Figure 4. a) Chronogram of the sequence used for self-diffusion measurement. θ represents a small flip angle pulse. The respective phases of the 90° pulses and of the receiver are (x), (x -x), (y -y x -x), (x x -x -x). Each NMR sequences starts after 10 seconds syringe push and 1 second waiting time. During the first loop l_1, the gradient strength increases linearly. It is reset to the initial value at each l_2 loop. b) Corresponding one-pulse spectra array, recorded after small flip angle pulse (θ = 7.5°). c) Hyperpolarized ^{129}Xe self-diffusion spectra array. Four loops of 16 gradient strength increasing values were acquired with Δ=5 ms and δ=0.75 ms.

In order to extract the diffusion coefficients (D) for the xenon sites, the sum of the signal intensities (S) of the first two loops for each peak were fitted, respectively, by using the following equation,

$$S = S_0 \exp(-bD) \qquad (3)$$

where $b = \gamma^2\delta^2g^2(\Delta\text{-}\delta/3)$, γ is the ^{129}Xe gyromagnetic ratio, g the gradient strength, while δ and Δ are the gradient duration and delay between gradients, respectively, as indicated in Fig. 4a.

The fitted results are shown in Table 1. The plots of measured and fitted signal intensity of signal F from Fig. 4c, as well as signals L and M as a function of b are shown in Fig. 5. The fitted diffusion coefficient of free Xe gas is 6.4 ± 0.6 10^{-6} m^2/s, corresponding to a previous study.[24] The Xe gas in large pore has diffusion coefficient of 2.8 ± 0.7 10^{-7} m^2/s and the ^{129}Xe gas in medium pore has smaller diffusion coefficient of 1.1 ± 0.4 10^{-8} m^2/s. Fig. S5, giving separately the diffusion curves for two successive loops, shows that the dispersion is low when the signal-to-noise ratio is high enough. It is reasonable to assume that when xenon gas remains in smaller pores, diffusion is restricted compared to that of the free gas or the gas in larger pores. In this case of restricted diffusion with small Δ values, with such a proven sequence, several Δ values could be employed with a single xenon batch, giving easier access to the surface-to-volume ratio.[25]

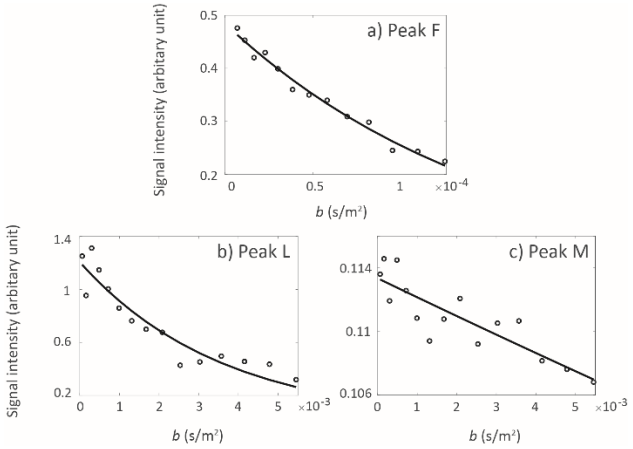

Figure 5. Sum of the normalized signal intensities of the first two self-diffusion loops (circles) plotted as a function of b and the fits (lines) by using equation (3): a) peak F evolution from the experiment with Δ=1.6 ms and δ=0.2 ms, b) peak L evolution from the experiment with Δ=1.6 ms and δ=0.2 ms and c) peak M evolution from the experiment with Δ=5 ms and δ=0.75 ms.

Table 1. Calibrated self-diffusion signal intensities obtained by fitting Eq. (3) on three signals: peak F (a) from the spectra with Δ=1.6 ms and δ=0.2 ms, as well as peak L (b) and peak M (c) from the spectra with Δ=5 ms and δ=0.75 ms.

Peak	S_0	D (m^2/s)
F	0.48 ± 0.015	(6.4 ± 0.6) * 10^{-6}
L	1.21 ± 0.13	(2.8 ± 0.7) * 10^{-7}
M	0.11 ± 0.0011	(1.1 ± 0.4) * 10^{-8}

^{129}Xe EXSY spectra. EXSY experiments were performed on the MCM-41 sample by either introducing thermally polarized ^{129}Xe gas in an NMR tube or using our stopped-flow system with hyperpolarized xenon. The TP ^{129}Xe EXSY spectra were performed with four mixing times, 0.2, 0.5, 5 and 100 ms for an experiment time of ca. 8 hours each (Fig. 6a, b display the contour plots for 5 and 100 ms) and HP ^{129}Xe EXSY spectra used five mixing times, 1, 5, 45, 70 and 100 ms for experiment time of ca. 2 min each (Fig. 6c, d display the contour plots for 5 and 100 ms). Note that in one xenon batch (use of one glass serpentine content) at least two mixing times could be recorded. Also, the quality of the gas flow stop and the fine-tuning of the 90° pulses by the methods described above make it possible to dispense with the use of coherence selection gradients. The latter, designed to suppress axial peaks among other effects, would introduce unavoidable diffusion filtering, greatly limiting the sensitivity of the experiment and biasing its quantitative aspect.

All of the four TP ^{129}Xe EXSY spectra show three peaks belonging to S, M and P/F on the diagonal. For a mixing time of 0.5 ms, the exchange peaks between peak M and F starts to appear. Exchange cross-peaks both between S and F and between S and M are observed at a mixing time of 100 ms. Note that the cross-peaks are very similar in intensity on either side of the diagonal, meaning that the flow is balanced. But the L signal is not observed due to its poor intensity with respect to the others. In contrast, EXSY experiments with hyperpolarized xenon have a high signal-to-noise ratio, and the four signals P/F, L, M and S are clearly visible. A net exchange is evidenced at a mixing time of 100 ms between signals L and M, and L-P as L-S cross-peaks are also observed, however of lower intensity.

As expected, the free xenon gas (F+P signal) exchanges faster with the gas in the hexagonal mesopores (M) than with the gas in the small pores (S) and in the large pores (L). For the latter this may be because the residual organic template hinders the gas exchange.

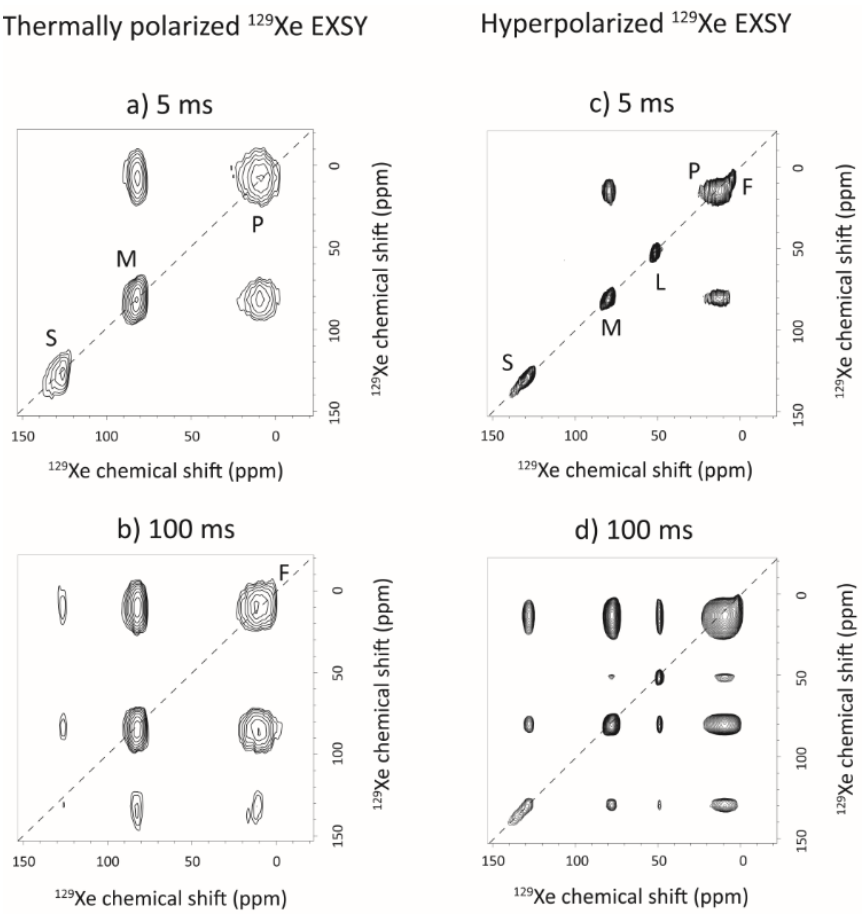

Figure 6. (a, b) TP ^{129}Xe EXSY NMR spectra, (c, d) HP ^{129}Xe EXSY NMR spectra. These last two experiments have been chained for the same xenon batch. 32 points constitute the indirect dimension of the TP ^{129}Xe experiments, while there are 48 points for the HP ^{129}Xe EXSY.

CONCLUSION

A low-cost device enabling dynamic introduction of hyperpolarized xenon in porous materials in continuous or stopped-flow mode for NMR studies is presented. It can be installed on different types of NMR magnets, as it is plugged onto a Bruker micro-imaging probe basis. It comprises a disposable flow NMR insert mainly built by additive manufacturing. Detection is made via a copper solenoid coil placed as close as possible to the porous material. Only small quantities of porous – volumes between 5 (with a second version of insert containing a chamber of 1 mm diameter) and 25 mm^3 - are required, which represents a great advantage for expensive materials. This simple device allows work in anhydrous mode, or the introduction of other gases in competition or before/after xenon. An efficient stopped-flow system based on two pneumatic valves controlled from the NMR sequence provides a clean shut-off of the gas flow. This enables 2D experiments such as ^{129}Xe self-diffusion and EXSY experiments to be carried out. With such a set-up, small quantities of rare gases are required and the xenon used can be easily recovered.

As a proof of concept, this device was used to study a model commercial porous material with multi-porosity. Thanks to the increased sensitivity of xenon hyperpolarization and the efficiency of this set-up, the study of gas diffusion and exchange between the various pores of the commercial MCM-41 sample has been facilitated. The presence of defect pores and micropores, undoubtedly due to the presence of template prior to calcination, has been evidenced.

T_1-T_2 correlation experiments, or any other experiment enabling finer characterization of the porous material, could now be the logical follow-up to these developments.

In addition, Xe/CO_2, Xe/Kr (or else) competition experiments, which are easy to perform with this set-up, will be of great interest for the study of the performances of other porous samples such as metal-organic frameworks. Changing the tuning capabilities of the probe is very easy in this set-up, making it possible to observe other nuclei without changing the porous material. Also temperature-dependent measurements could be used to derive an activation energy for Xe exchange between different sites.

EXPERIMENTAL SECTION

NMR experiments with thermal xenon. For experiments with thermally-polarized (TP) xenon, the commercial MCM-41 powder (ref. 643645-5G from Sigma-Aldrich, France) was introduced into a 5-mm NMR glass tube. Then about 1.5 atm of xenon gas enriched at 83% in isotope 129 (Eurisotop, France) was condensed into tube by using a vacuum line and liquid N_2. ^{129}Xe single pulse and EXSY experiments were performed at 294 K on this sample on a Bruker Avance II spectrometer (Bruker, Billerica, MA, USA) equipped with a 5 mm BBO probe. The ^{129}Xe 90° pulse was 7 µs at 75 W. The one-pulse experiment was set with 640 scans and interscan delay of 5 s. The TP ^{129}Xe EXSY spectra were collected with varying mixing times of 0.2, 0.5, 5 and 100 ms, respectively. The number of scans was 160 and the relaxation recovery delay was 5 s. The size of the indirect dimension was 32. The experiment time of each EXSY spectra was ca. 8 h (depending on the mixing time).

Building of the NMR insert via 3D-printing. The piece was conceived and drawn in SolidWorks (Dassault Systèmes, France) and built on an Objet 30 Pro polyjet printer (Stratasys, USA), using VeroClear resin. The STL files can be found at https://github.com/LSDRM/StopFlow-PorousNMR.

Preparation of the sample for the stopped-flow device. The porous material is manually inserted in the 3D-printed insert, and then gently compacted with a small ceramic pestle. To avoid too much settling during this manual stage, pressure gauges (see below) are very important. A 3D-printed cap is then screwed on. Its design leaves the gas path free even when fully tightened.

Production of hyperpolarized xenon and details on the stopped-flow xenon injection device operation. Xenon enriched at 83% in isotope 129 (Eurisotop, France) was hyperpolarized through spin-exchange optical pumping[2] in the batch mode using an experimental setup already described.[26] To inject the hyperpolarized ^{129}Xe gas, nitrogen gas contained into a 140 mL plastic syringe is pushed by a programmable non-magnetic syringe pump (Harvard Apparatus PHD2000, USA) in a vacuum line. The syringe driver is connected to the TTL output of the spectrometer in order to trigger the gas injection with the pulse program. Nitrogen pushes the ^{129}Xe gas inside a connected glass solenoid placed on the top of the 11.7 T narrow bore NMR magnet. In order to rapidly stop and restart the gas flow a system of pneumatic valves (model PMDP-3-M6KG from Takasago, Japan) is used. They are positioned upstream and downstream of the NMR detection zone, enabling the flow to be stopped almost immediately and keeping the gas atmosphere at the both ends of the sample. These two membrane valves are controlled with 6 bar pressure controlled via a 3/2-inch electro-valve (Festo 7802 MFH-2-1/8, Germany) far from the NMR magnet field controlled by the TTL output of the spectrometer.

To monitor and debug the system, two pressure sensors (ABP2MANT010BAAA5XX) are present, right before the Xe container and after the porous along the gas flow. They are embedded on a homemade data-acquisition board (DAB), where an UART controlled ADC (ADS122U04) sends pressure data to a computer, on which a GUI enables one to record and plot them. The DAB is just lying on top of the NMR spectrometer. Communication between the DAB and the computer, 10 meters apart, uses UART protocol with RS-485 standard, which allows high speed and long distances even in high EMF environment. A USB to UART RS-485 module using the bridge chip (FT231XS) and an RS-485 transceiver (MAX14840EATA+) allow the computer to

communicate through the line. This configuration works well, but the use of RS-422 may be consider instead of RS-485, for improving robustness and optimization of the data transfer rates while minimizing errors. A thermocouple connector is also mounted on the DAB in the aim of measuring temperature as close as possible to the porous, since the classical thermocouple (PIT) inside the probehead is rather far from the sample and the temperature inertia between the PIT and the porous is high. The DAB-mounted thermocouple was not used in the described experiments, since no fine temperature characterization was needed. The DAB is powered with a standard 24 V continuous source (RS PRO 175-3306), regulated through a power regulation stage. The used GUI had been thought and designed in the aim of being very versatile and usable with as much configurations as possible. It allows measurements to be traced and recorded, and actuators to be controlled manually or automatically according to set parameters. Instructions can be found at https://github.com/LSDRM/VMCGUI while description of the designed electronic boards can be found at https://github.com/LSDRM/VMC_Kits/tree/main/Customized/DualPressure-Thermocouple_forVMCGUI.

Figs. S1 and S2 show the designed electronic boards.

Self-diffusion and EXSY experiments with hyperpolarized xenon (see https://github.com/LSDRM/StopFlow-PorousNMR). A stimulated spin-echo sequence containing the commands for the stopped-flow system and interleaved with a single acquisition made of a small flip angle read pulse was used for self-diffusion experiments (see Fig. 4 and Fig. S6). Between two consecutive scans, the xenon was pushed for 1 second (rate 10 mL/min). The stabilization time after xenon thrust was 0.2 s, the number of scans was 2. Diffusion was encoded along the z direction, i. e. perpendicular to the xenon flow.

The HP ^{129}Xe EXSY spectra were collected with varying mixing times of 1, 5, 45, 70 and 100 ms, respectively, using a home-made sequence containing the commands for the stopped-flow system (shown in Fig. S7). Between two consecutive scans, the xenon was pushed for 1 second (rate 5mL/min). The stabilization time after xenon thrust was 0.2 s, the number of scans was 2. The size of the indirect dimension was 48. The experiment time of each EXSY spectra was thus ca. 2 min (depending on the mixing time). States-TPPI mode was used in the indirect dimension.

ASSOCIATED CONTENT

Supporting Information

Electronic boards of pressure sensors, N_2 sorption data, hyperpolarized ^{129}Xe continuous flow spectra and Topspin pulse programs (PDF).

AUTHOR INFORMATION

Corresponding Author

*** Patrick Berthault − NIMBE, CEA, CNRS, Université de Paris Saclay, CEA Saclay, 91191 Gif-sur-Yvette, France; Email:** patrick.berthault@cea.fr

Authors

Jing Li − NIMBE, CEA, CNRS, Université de Paris Saclay, CEA Saclay, 91191 Gif-sur-Yvette, France

Estelle Léonce − NIMBE, CEA, CNRS, Université de Paris Saclay, CEA Saclay, 91191 Gif-sur-Yvette, France

Corentin Coutellier − NIMBE, CEA, CNRS, Université de Paris Saclay, CEA Saclay, 91191 Gif-sur-Yvette, France

Céline Boutin − NIMBE, CEA, CNRS, Université de Paris Saclay, CEA Saclay, 91191 Gif-sur-Yvette, France

Kévin Chighine − NIMBE, CEA, CNRS, Université de Paris Saclay, CEA Saclay, 91191 Gif-sur-Yvette, France

Charles Rivron − NIMBE, CEA, CNRS, Université de Paris Saclay, CEA Saclay, 91191 Gif-sur-Yvette, France

Anne Davidson − Laboratoire de Réactivité de Surface, Sorbonne Universités, UPMC Université Paris 06, UMR CNRS 7197, 4 Place Jussieu, 75005 Paris, France

Author Contributions

The manuscript was written through contributions of all authors. All authors have given approval to the final version of the manuscript.

Notes

The authors declare no competing financial interest.

ACKNOWLEDGMENT

Support from the French Ministry of Research (project ANR-20-CE30-0021 HELPING) is acknowledged, in particular for the financing of the post-doctoral internship of JL.

REFERENCES

(1) Ito, T.; Fraissard, J. 129Xe NMR Study of Xenon Adsorbed on Y Zeolites. *J. Chem. Phys.* **1982**, *76*, 5225–5229.

(2) Walker, T. G. Fundamentals of Spin-Exchange Optical Pumping. *J. Phys.: Conf. Ser.* **2011**, *294*, 012001.

(3) Comment, A.; Jannin, S.; Hyacinthe, J.-N.; Miéville, P.; Sarkar, R.; Ahuja, P.; Vasos, P. R.; Montet, X.; Lazeyras, F.; Vallée, J.-P.; Hautle, P.; Konter, J. A.; Van Den Brandt, B.; Ansermet, J.-Ph.; Gruetter, R.; Bodenhausen, G. Hyperpolarizing Gases via Dynamic Nuclear Polarization and Sublimation. *Phys. Rev. Lett.* **2010**, *105*, 018104.

(4) Kemnitzer, T. W.; Tschense, C. B. L.; Wittmann, T.; Rössler, E. A.; Senker, J. Exploring Local Disorder within CAU-1 Frameworks Using Hyperpolarized 129Xe NMR Spectroscopy. *Langmuir* **2018**, *34*, 12538–12548.

(5) Nossov, A.; Haddad, E.; Guenneau, F.; Gédéon, A. Application of Continuously Circulating Flow of Hyperpolarized (HP) 129Xe-NMR on Mesoporous Materials. *Phys. Chem. Chem. Phys.* **2003**, *5*, 4473–4478.

(6) Sears, D. N.; Demko, B. A.; Ooms, K. J.; Wasylishen, R. E.; Huang, Y. Formation of Porous Aluminophosphate Frameworks Monitored by Hyperpolarized ^{129} Xe NMR Spectroscopy. *Chem. Mater.* **2005**, *17*, 5481–5488.

(7) Liu, Y.; Zhang, W.; Xie, S.; Xu, L.; Han, X.; Bao, X. Probing the Porosity of Cocrystallized MCM-49/ZSM-35 Zeolites by Hyperpolarized ^{129}Xe NMR. *J. Phys. Chem. B* **2008**, *112*, 1226–1231.

(8) Simonutti, R.; Bracco, S.; Comotti, A.; Mauri, M.; Sozzani, P. Continuous Flow Hyperpolarized 129Xe NMR for Studying Porous Polymers and Blends. *Chem. Mater.* **2006**, *18*, 4651–4657.

(9) Knagge, K.; Smith, J. R.; Smith, L. J.; Buriak, J.; Raftery, D. Analysis of Porosity in Porous Silicon Using Hyperpolarized 129Xe Two-Dimensional Exchange Experiments. *Solid State Nucl. Magn. Reson.* **2006**, *29*, 85–89.

(10) Wang, L.-Q.; Wang, D.; Liu, J.; Exarhos, G. J.; Pawsey, S.; Moudrakovski, I. Probing Porosity and Pore Interconnectivity in Crystalline Mesoporous TiO2 Using Hyperpolarized 129Xe NMR. *J. Phys. Chem. C* **2009**, *113*, 6577–6583.

(11) Causier, A.; Carret, G.; Boutin, C.; Berthelot, T.; Berthault, P. 3D-Printed System Optimizing Dissolution of Hyperpolarized Gaseous Species for Micro-Sized NMR. *Lab Chip* **2015**, *15*, 2049–2054.

(12) Carret, G.; Berthelot, T.; Berthault, P. Enhancing NMR of Nonrelaxing Species Using a Controlled Flow Motion and a Miniaturized Circuit. *Anal. Chem.* **2017**, *89*, 2995–3000.

(13) McDonnell, E. E.; Han, S.; Hilty, C.; Pierce, K. L.; Pines, A. NMR Analysis on Microfluidic Devices by Remote Detection. *Anal. Chem.* **2005**, *77*, 8109–8114.

(14) Kresge, C. T.; Leonowicz, M. E.; Roth, W. J.; Vartuli, J. C.; Beck, J. S. Ordered Mesoporous Molecular Sieves Synthesized by a Liquid-Crystal Template Mechanism. *Nature* **1992**, *359* (6397), 710–712.

(15) Bhattacharyya, S.; Lelong, G.; Saboungi, M.-L. Recent Progress in the Synthesis and Selected Applications of MCM-41: A Short Review. *J. Exp. Nanosci.* **2006**, *1*, 375–395.

(16) Dündar-Tekkaya, E.; Yürüm, Y. Mesoporous MCM-41 Material for Hydrogen Storage: A Short Review. *Int. J. Hydrogen Energy* **2016**, *41*, 9789–9795.

(17) Huang, S.-J.; Huang, C.-H.; Chen, W.-H.; Sun, X.; Zeng, X.; Lee, H.-K.; Ripmeester, J. A.; Mou, C.-Y.; Liu, S.-B. Probing the Alkyl Ligands on Silylated Mesoporous MCM-41 Using Hyperpolarized ^{129}Xe NMR Spectroscopy. *J. Phys. Chem. B* **2005**, *109*, 681–684.

(18) Zhang, W.; Ratcliffe, C. I.; Moudrakovski, I. L.; Mou, C.-Y.; Ripmeester, J. A. Distribution of Gallium Nanocrystals in Ga/MCM-41 Mesocomposites by Continuous-Flow Hyperpolarized ^{129}Xe NMR Spectroscopy. *Anal. Chem.* **2005**, *77*, 3379–3382.

(19) Frasch, J.; Lebeau, B.; Soulard, M.; Patarin, J.; Zana, R. In Situ Investigations on Cetyltrimethylammonium Surfactant/Silicate Systems, Precursors of Organized Mesoporous MCM-41-Type Siliceous Materials. *Langmuir* **2000**, *16*, 9049–9057.

(20) Fraissard, J.; Ito, T. 129Xe n.m.r. Study of Adsorbed Xenon: A New Method for Studying Zeolites and Metal-Zeolites. *Zeolites* **1988**, *8*, 350–361.

(21) Ripmeester, J. A.; Ratcliffe, C. I. 129Xe NMR Spectroscopy in Microporous Solids: The Effect of Bulk Properties. *Anal. Chim. Acta* **1993**, *283*, 1103–1112.

(22) Lin, H.-P.; Wong, S.-T.; Mou, C.-Y.; Tang, C.-Y. Extensive Void Defects in Mesoporous Aluminosilicate MCM-41. *J. Phys. Chem. B* **2000**, *104*, 8967–8975.

(23) Norquay, G.; Leung, G.; Stewart, N. J.; Wolber, J.; Wild, J. M. ^{129}Xe Chemical Shift in Human Blood and Pulmonary Blood Oxygenation Measurement in Humans Using Hyperpolarized ^{129}Xe NMR: Noninvasive Measurement of Pulmonary Blood Oxygenation. *Magn. Reson. Med.* **2017**, *77*, 1399–1408.

(24) Mair, R. W.; Cory, D. G.; Peled, S.; Tseng, C.-H.; Patz, S.; Walsworth, R. L. Pulsed-Field-Gradient Measurements of Time-Dependent Gas Diffusion. *J. Magn. Reson.* **1998**, *135*, 478–486.

(25) Latour, L. L.; Mitra, P. P.; Kleinberg, R. L.; Sotak, C. H. Time-Dependent Diffusion Coefficient of Fluids in Porous Media as a Probe of Surface-to-Volume Ratio. *J. Magn. Reson. Ser. A* **1993**, *101*, 342–346.

(26) Chauvin, C.; Liagre, L.; Boutin, C.; Mari, E.; Léonce, E.; Carret, G.; Coltrinari, B.; Berthault, P. Spin-Exchange Optical Pumping in a Van. *Rev. Sci. Instrum.* **2016**, *87*, 016105.

GRAPHICAL TOC